A Low-Complexity CLSIC-LMMSE-Based Multi-User Detection Algorithm for Coded MIMO Systems with High Order Modulation

Jin Xu[1], Kai Zhang[2]
[1]School of Computer and Communication Engineering, Zhengzhou University of Light Industry, Zheng Zhou, China 450000
[2] School of Information and Communication Engineering, Beijing University of Posts and Telecommunications, Bei Jing, China 100876
[e-mail:buptxujin@163.com, zk510@163.com]
*Corresponding author: Jin Xu

Received August 3, 2016; revised December 25, 2016; accepted February 14, 2017; published April 30, 2017

Abstract

In this work, first, a multiuser detection (MUD) algorithm based on component-level soft interference cancellation and linear minimum mean square error (CLSIC-LMMSE) is proposed, which can enhance the bit error ratio (BER) performance of the traditional SIC-LMMSE-based MUD by mitigating error propagation. Second, for non-binary low density parity check (NB-LDPC) coded high-order modulation systems, when the proposed algorithm is integrated with partial mapping, the receiver with iterative detection and decoding (IDD) achieves not only better BER performance but also significantly computational complexity reduction over the traditional SIC-LMMSE-based IDD scheme. Extrinsic information transfer chart (EXIT) analysis and numerical simulations are both used to support the conclusions.

Keywords: multiple-input multiple-output, component-level soft interference cancellation, non-binary LDPC, iterative detection and decoding, extrinsic information transfer chart

A preliminary version of this paper appeared in IEEE VTC2014-Fall, Sep. 14-17, Vancouver, Canada. This version includes a concrete analysis and supporting implementation results on CLSIC-LMMSE-IDD. This work has been partly supported by National Natural Sicence Foundation of China(Grant No. 61601411) and 863 project of China (No. SS2014AA012105).

https://doi.org/10.3837/tiis.2017.04.007 **ISSN : 1976-7277**

1. Introduction

Orthogonal multiple access (OMA) is preferred in traditional cellular wireless communication systems since that a low complexity detection algorithm is sufficient to achieve promising performance at the receiver side. In this paper, we consider orthogonal freqency division multiplexing (OFDM) based uplink multi-user multiple-input multiple-output (MU-MIMO) system with high order modulation [1]. The motivation to consider such MU-MIMO system is its potential to meet the growing demands for higher throught and spectral efficiency for future fifth generation (5G) mobile systems. As the existence of multiuser interference at the base station (BS), one key issue in the design of a practical receiver for uplink MU-MIMO system with high order modulation is how to reduce the complexity of the detection algorithm without much compromise in performance.

Among all soft-input soft-output (SISO) MU-MIMO detection algorithms, the maximum *a posteriori* (MAP) algorithm achieves the best performance [2-3], however its computational complexity increases exponentially with the number of transmit antennas and the constellation size. To reduce the detection complexity, several efforts are dedicated to the development of suboptimal detectors. Linear detectors (such as zero forcing (ZF) or minimum mean square error (MMSE)) have low computational complexity but the performances of these algorithms are far inferior to the maximum-likelihood (ML) algorithm. Ordered soft interference cancellation (OSIC) based LMMSE detection achieves a tradeoff between complexity and performance, which is suitable for complexity-limited applications [4]. Furthermore, by iterative detection and decoding (IDD) technology which exchanges the soft information between the detector and the channel decoder iteratively, successive interference cancellation and LMMSE filtering (SIC-LMMSE) based receiver can be further enhanced [5]. The key idea underlying the SIC-LMMSE base IDD algorithm is that SIC-LMMSE detector compute the estimates of the transmitted symbols based on the *a priori* Log-likelihood ratios (LLRs) fedback from channel decoder. Those estimates are then utilized to compute soft symbols and are cancelled as interference from the received signal. The residual interference plus noise is equalized using the LMMSE filter, followed by a computation of the *a posteriori* LLRs per stream. However, the performance of the SIC-LMMSE base IDD is prone to error propagation (EP), which arises in any receiver using decision-feedback. To overcome this problem, it is shown that incorporating soft decisions into the decision feedback process is an effective way of mitigating EP [6]. In [6], the soft input soft output with feedback (SIOF) V-BLAST detector is proposed to mitigate EP, and we prefer to call this algorithm symbol-level soft interference cancellation (SLSIC) based LMMSE (SLSIC-LMMSE) detection due to that the algorithm opterate detection and cancellation on symbol level. The key points of SLSIC-LMMSE algorithm are the following two aspects: 1) the SLSIC-LMMSE-based detector subtracts the *a priori* estimates of the undetected layers and subtracts an *a posteriori* estimates of the previously detected layers. This method delivers better detection performance since the *a posteriori* information generally provides an additional information than the *a priori* information, and 2) the symbols can be detected one by one and the detection ordering is determined according to the symbol-wise MSE metric.

In this paper, by exploiting the independence between the in-phase and quadrature components (I/Q), a component level soft interference cancellation based LMMSE (CLSIC-LMMSE) MUD algorithm is proposed to enhance the performance of the traditional SLSIC based one. Since the two quadrature components of the modulation symbol can be separately

detected (operated on component level) and then be used to aid the interference cancellation operation, we prefer to call the proposed algorithm CLSIC-LMMSE detection.

High order modulation is a bandwidth-efficient scheme for digital communication systems. Non-binary LDPC coded high order modulation scheme shows capacity-approaching performance over both additive white Gaussian noise (AWGN) and Rayleigh fading channels [7, 2]. However, a practical challenge is the decoding complexity increases with the square of the order of the Galois field (GF) [8].

In this work, an IDD scheme that combines non-binary LDPC decoding with CLSIC-LMMSE detection is proposed for coded MU-MIMO system with high order modulation, where the order of in-phase or quadrature component of the quadrature amplitude modulation (QAM) symbol equal to GF order. Furthermore, a partial mapping scheme is employed to reduce the computation complexity of the non-binary LDPC decoding [9]. The main contributions of this paper are summarized as follows: 1) a partial mapping from non-binary LDPC code over low order GF to the I/Q componet of QAM symbol is presented to reduce the decoding computational complexity, 2) a novel CLSIC-LMMSE detection algorithm is derived and combined with the proposed partial mapping scheme seemlessly. 3) non-binary AMI chart is employed to illustrate the advantages of the proposed algorithm.

2. System Model

2.1 System model of coded MU-MIMO system

Consider a turbo/non-binary LDPC coded uplink MU-MIMO system with N_t independent users, where each user equipped with one transmit antenna, and the receiver equipped with N_r antennas. As shown in **Fig. 1**, the transmission scheme for each user ultilizes OFDM to combat intersymbol interference, and IDD structure is emploed at the receiver.

For coded MIMO system with 2m-ary quadrature amplitude modulation (QAM), two cases are considered. One employs binary turbo, in which each m coded bits are mapped to one modulation symbol. the other one adopts the non-binary LDPC codes, in which the symbol mapping and partial mapping are employed for traditional scheme and the proposed scheme respectively. The detailed mapping schemes are depicted in Fig. 2. For $1 \le k \le N_t$, the frequency domain symbol of the *k*-th user at a speicfic subcarrier is denoted by x_k, where $x_k \in \mathcal{A}$. Let $\mathbf{x}_c \in C^{N_t \times 1}$ denote the symbol vector transmitted simutaneously by all users at a specific subcarrier, each element of $\mathbf{x}_c = [x_1, \cdots, x_{N_t}]^T$ belongs to a specific user and belongs to the QAM constellation $\mathcal{A}$. At the receiver, it is assume that the N_t transmitters and the reciver are synchoronized and all channel coefficients are known. The received signal $\mathbf{y}_c$ at a association subcarrrier can be written as

$$\mathbf{y}_c = \mathbf{H}_c \mathbf{x}_c + \mathbf{n}_c \tag{1}$$

where $\mathbf{H}_c$ denotes the channel gain matrix, the elements of which obtained from an independent identically distributed (i.i.d) complex Gaussian distribution with zero mean and unit variance. $\mathbf{n}_c \in C^{N_r \times 1}$ is the noise vector whose entries are modeled as i.i.d $CN(0, N_t E_s / \rho)$, where E_s is the average energy of transmitted symbols, and ρ is the average signal-to-noise

ratio (SNR) received by each receiving antenna. As in [3], we define single user average bit signal to noise ratio E_b/N_0 as follows:

$$\left(\frac{E_b}{N_0}\right)_{dB} = \left(\frac{E_s}{N_0}\right)_{dB} + 10\log_{10}\left(\frac{N_r}{R_c m}\right) \tag{2}$$

where R_c denotes the channel coding rate and *m* denotes the number of bits corresponding to each constellation point.

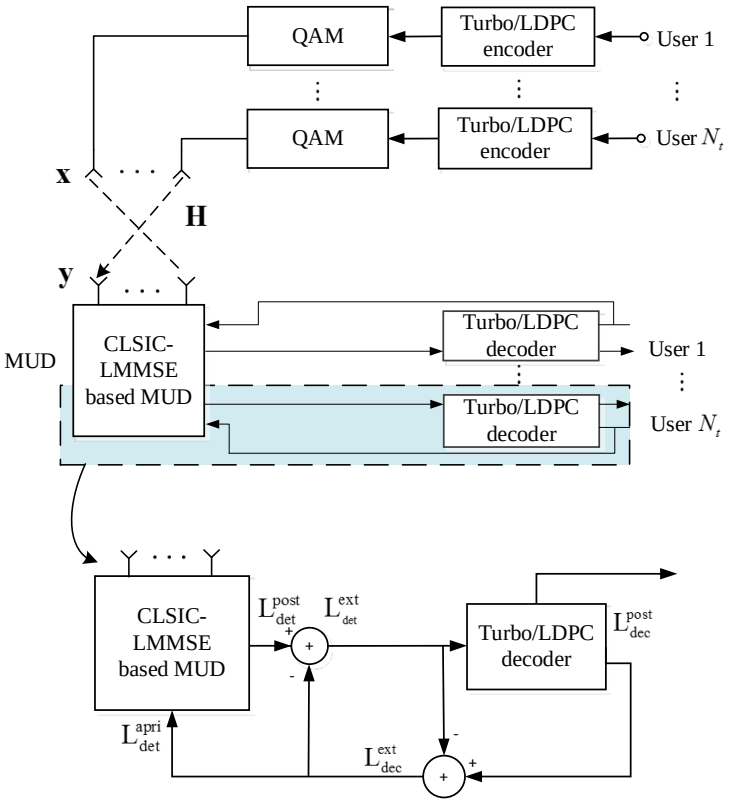

Fig. 1. System model

2.2 Partial mapping for the proposed CLSIC-LMMSE MUD algorithm

For binary turbo coded MIMO system, no matter which MUD algorithm is used, the mapping scheme is the same. For traditional non-binary LDPC coded high order modulation system, it is obviously to employ symbol mapping, which mapping each non-binary LDPC code symbol to one constellation point. Take 16-QAM system for example, each GF(2^4)-LDPC symbol can directly be mapped onto one constellation point, as depicted in **Fig. 2(a)**. At the receiver, one complex-valued symbol can be detected and canceled at every turn with SLSIC-LMMSE detection algorithm [5-6]. The above scheme is referred to as traditional scheme in this paper. Partial mapping was first presented in [9] for non-binary LDPC code QAM system in AWGN channel to reduce the decoding complexity. In this paper, for non-binary LDPC coded MIMO

system, we proposed combining partial mapping with CLSIC-LMMSE-based MUD algorithm to achieve low complexity and high performance of IDD receiver. Similarly, take 16-QAM system for example, each GF(2^2)-LDPC symbol is mapped onto the in-phase or quadrature component of a 16-QAM symbol, as depicted in **Fig. 2(b)**. At the receiver side, CLSIC-LMMSE based detection is performed. The extension to 64QAM case is straightforward.

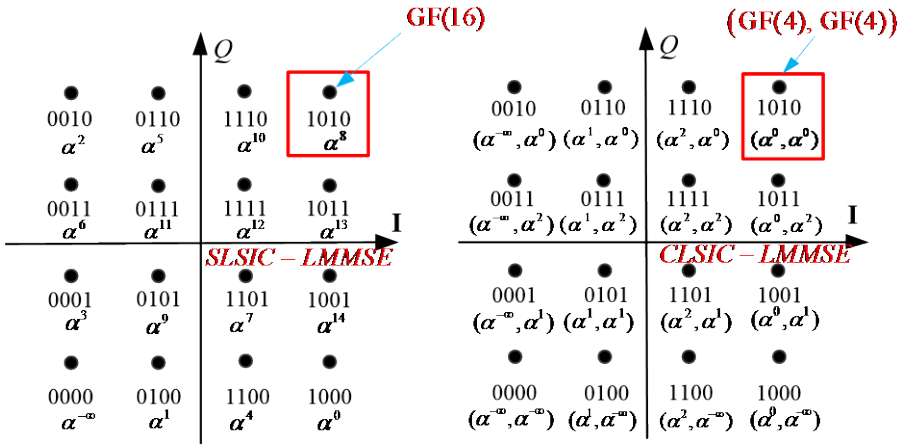

(a) symbol mapping **(b) partial mapping**

Fig. 2. Cosntellation mapping for both schemes

2.3 Real-value expression for MU-MIMO system

To perform the CLSIC-LMMSE based detection, the complex model (1) should be converted into a real-valued expression as follows:

$$\mathbf{y} = \mathbf{H}\mathbf{x} + \mathbf{n} \tag{3}$$

where $\mathbf{H} \in R^{2N_r \times 2N_t}$, $\mathbf{y} \in R^{2N_t \times 1}$, $\mathbf{x} \in R^{2N_t \times 1}$, $\mathbf{n} \in R^{2N_t \times 1}$, and equivalently we have

$$\mathbf{y} = \begin{bmatrix} \mathrm{Re}(\mathbf{y}_c) \\ \mathrm{Im}(\mathbf{y}_c) \end{bmatrix}, \ \mathbf{H} = \begin{bmatrix} \mathrm{Re}(\mathbf{H}_c) & -\mathrm{Im}(\mathbf{H}_c) \\ \mathrm{Im}(\mathbf{H}_c) & \mathrm{Re}(\mathbf{H}_c) \end{bmatrix}, \mathbf{x} = \begin{bmatrix} \mathrm{Re}(\mathbf{x}_c) \\ \mathrm{Im}(\mathbf{x}_c) \end{bmatrix}, \ \mathbf{n} = \begin{bmatrix} \mathrm{Re}(\mathbf{n}_c) \\ \mathrm{Im}(\mathbf{n}_c) \end{bmatrix}.$$

3. Proposed CLSIC-LMMSE based MUD

3.1 LMMSE filtering with CLSIC

In this subsection, we illustrate the details of the proposed CLSIC-LMMSE-based MUD detection algorithm. Assume x_k is the *k*-th symbol to be detected. Let $\mathbf{S}_D = [x_0, \cdots, x_{k-1}]$ denote the set of detected symbols, whereas $\mathbf{S}_A = [x_{k+1}, \cdots, x_{2N_t}]$ denotes the set of undetected symbols. The CLSIC-LMMSE contains two steps during each iteration, one is the LMMSE filtering, the other is soft interference cancellation. Following [5-6], the LMMSE estimate of x_k, denoted by $\hat{x}_k$, can be obtained by multiplying y_k with the LMMSE weight vector w_k as follows:

$$\hat{x}_k = \mathbf{w}_k^{\mathrm{T}} \mathbf{y}_k \tag{4}$$

The component-level soft interference cancellation (CLSIC) process can be depicted as follows

$$\mathbf{y}_k = \mathbf{y} - \mathbf{H} \begin{bmatrix} \overline{\boldsymbol{\gamma}}_{k-1} \\ 0 \\ \overline{\boldsymbol{\gamma}}_{k+1} \end{bmatrix} \tag{5}$$

where $\overline{\boldsymbol{\gamma}}_{k-1} = [\mathrm{E}(x_1 \mid \mathbf{L}_1^{post}), \cdots, \mathrm{E}(x_{k-1} \mid \mathbf{L}_{k-1}^{post})]^T$, $\overline{\boldsymbol{\gamma}}_{k+1} = [\mathrm{E}(x_{k+1} \mid \mathbf{L}_{k+1}^{apri}), \cdots, \mathrm{E}(x_{2N_t} \mid \mathbf{L}_{2N_t}^{apri})]^T$. It should be noted that for arbitrary $1 \le i \le k-1$, i.e. $x_i \in S_D$, $\mathrm{E}(x_i \mid \mathbf{L}_i^{post})$ should be calculated from its associated *a posterior* LLRs which obtained from the previously detected *k*-1 symbols, whereas for $k+1 \le i \le 2N_t$, i.e. $x_i \in S_A$, $\mathrm{E}(x_i \mid \mathbf{L}_i^{apri})$ should be calculated from its associated *a prior* LLRs which obtained from the channel decoder, both as depicted in (11). $\mathrm{E}(x_i \mid \mathbf{L}_i^{apri})$ should be set to zero at the first iteration. The LMMSE filtering vector can be obtained according to

$$\mathbf{w}_k = \arg\min_{\mathbf{w}} \mathrm{E}[(x_k - \mathbf{w}^T \mathbf{y}_k)^2] \tag{6}$$

thus, we get

$$\mathbf{w}_k = \left(\mathbf{H}\mathbf{V}_x\mathbf{H}^T + \sigma_n^2 \mathbf{I}_{2N_t}\right)^{-1} \mathbf{h}_k \, \mathrm{var}(x_k) \tag{7}$$

where

$$\mathbf{V}_x = \begin{bmatrix} \mathbf{R}_{1:k-1}^{post} & 0 & 0 \\ 0 & 0.5 & 0 \\ 0 & 0 & \mathbf{R}_{k+1:2N_t}^{apri} \end{bmatrix} \tag{8}$$

In (8), the *k*-th diagonal term of matrix $\mathbf{V}_x$ is fixed to 0.5 during the calculation of x_k. $\mathbf{R}_{1:k-1}^{post} = diag(R_1^{post}, R_2^{post} \cdots R_{k-1}^{post})$ represents the covariance matrix of $[x_1, \cdots, x_{k-1}]^T$ and can be computed from the associated *a posteriori* LLRs of those symbols. $\mathbf{R}_{k+1:2N_t}^{apri} = diag(R_{k+1}^{apri}, R_{k+2}^{apri} \cdots R_{2N_t}^{apri})$ represents the covariance matrix of $[x_{k+1}, \cdots, x_{2N_t}]^T$ and can be computed from the corresponding *a priori* LLRs as expressed in (9) and (10). Since the in-phase and quadrature components of a QAM symbol are independent, $\mathbf{R}_{1:k-1}^{post}$ and $\mathbf{R}_{k+1:2N_t}^{apri}$ in (8) are diagonal matrices. Take the calculation of the *i*-th diagonal term of $\mathbf{R}_{1:k-1}^{post}$ or $\mathbf{R}_{k+1:2N_t}^{apri}$ for example,

$$R_i^{flag} = \mathrm{E}[x_i^2 \mid \mathbf{L}_i^{flag}] - \left(\mathrm{E}[x_i \mid \mathbf{L}_i^{flag}]\right)^2 \tag{9}$$

$$flag = \begin{cases} post & 1 \le i < k \\ apri & k < i \le 2N_t \end{cases} \tag{10}$$

The estimate of x_k can be rewritten as:

$$\hat{x}_k = \mathbf{w}_k^T \mathbf{y}_k = \tau x_k + z \tag{11}$$

where $\tau = \boldsymbol{w}_k^T \boldsymbol{h}_k$, $z = \boldsymbol{w}_k^T \left(\sum_{j=1, j \ne k}^{2N_t} \boldsymbol{h}_j \left(x_j - \mathrm{E}\left(x_j \right) \right) + \mathbf{n} \right)$, the covariance of z in equation (11) can be

calculated as $\sigma_z^2 = \mathrm{E}\left(zz^T\right) = \mathrm{var}\left(x_k\right)\boldsymbol{w}_k^T\left(\sum_{j=1,\, j\neq k}^{2N_t}\boldsymbol{h}_j\boldsymbol{h}_j^T\,\mathrm{var}\left(x_j\right) + \sigma_n^2\mathbf{I}_{2N_t}\right)\boldsymbol{w}_k$.

3.2 Bit-wise LLRs computation

For binary turbo coded MIMO system, $\mathrm{E}\left[x_i \mid \mathbf{L}_i^{flag}\right]$ and $\mathrm{E}\left[x_i^2 \mid \mathbf{L}_i^{flag}\right]$ in equation (8) can be alternatively written as $\mathrm{E}\left[x_i \mid \mathbf{L}_{i,1:Q}^{flag}\right]$ and $\mathrm{E}\left[x_i^2 \mid \mathbf{L}_{i,1:\mathrm{Q}}^{flag}\right]$,

$$\mathrm{E}\left[x_i \mid \mathbf{L}_{i,1:Q}^{flag}\right] = \sum_{\alpha=0}^{2^Q-1}\lambda_a \mathrm{Prob}\left[x_i = \lambda_a\right] \tag{12}$$

and

$$\mathrm{E}\left[x_i^2 \mid \mathbf{L}_{i,1:\mathrm{Q}}^{flag}\right] = \sum_{\alpha=0}^{2^Q-1}\lambda_\alpha^2 \mathrm{Prob}\left[x_i = \lambda_\alpha\right] \tag{13}$$

where $\mathbf{L}_{i,1:Q}^{flag}=[L_{i,1}^{flag}, L_{i,2}^{flag}\cdots L_{i,Q}^{flag}]$ denotes the LLR values of the Q bits associated with symbol x_i, and

$$\mathrm{Prob}\left[x_i = \lambda_\alpha\right] = \prod_{\beta=1}^{Q}\frac{\exp(\frac{1}{2}\mu_\beta L_{i,\beta})}{\exp(\frac{1}{2}L_{i,\beta}) + \exp(-\frac{1}{2}L_{i,\beta})} \tag{14}$$

where $\mu_\beta \in \{\pm 1\}$ and $\mu_\beta = 2c_\beta - 1$, $[c_1,\cdots,c_Q] = \chi^{-1}(\lambda_a)$ denotes the Q binary bits associated with symbol λ_a. After LMMSE filtering as shown in (4), we obtain an equivalent single input single ouptut model as (10). The *a posteriori* LLR of the $\beta - th$ $(1 \le \beta \le Q)$ bit associated with the symbol x_k can be calculated as follows:

$$L_{k,\beta}^{post} \approx \max_{\theta\in\chi_{k,\beta}^{(0)}}\left(-\frac{(\hat{x}_k - \tau\theta)^2}{2\sigma_z^2} + \sum_{\beta}\frac{1}{2}\mu_\beta L_{k,\beta}\right) - \max_{\theta\in\chi_{k,\beta}^{(1)}}\left(-\frac{(\hat{x}_k - \tau\theta)^2}{2\sigma_z^2} + \sum_{\beta}\frac{1}{2}\mu_\beta L_{k,\beta}\right) \tag{15}$$

where $\chi_{k,\beta}^{(0)}$ and $\chi_{k,\beta}^{(1)}$ stand for the set of 2^{Q-1} candidate symbols corresponding to $x_{k,\beta}=0$ and $x_{k,\beta}=1$ respectively. Then, the extrinsic LLR is obtained as

$$L_{k,\beta}^{ext} = L_{k,\beta}^{post} - L_{k,\beta}^{priori} \tag{16}$$

3.3 Component-wise LLR computation

For non-binary LDPC coded MIMO system, $\mathrm{E}\left[x_i \mid \mathbf{L}_i^{flag}\right]$ and $\mathrm{E}\left[x_i^2 \mid \mathbf{L}_i^{flag}\right]$ in equation (8) can be written as

$$\begin{aligned}\mathrm{E}\left[x_i \mid \mathbf{L}_i^{flag}\right] &= \sum_{\alpha=0}^{q-1}\lambda_a \mathrm{Prob}\left[x_i = \lambda_a\right] \\ &= \frac{\sum_{s=0}^{q-1}\lambda_s \exp\left(L_{i,s}\right)}{\sum_{t=0}^{q-1}\lambda_t \exp\left(L_{i,\mathrm{t}}\right)}\end{aligned} \tag{17}$$

and

$$\begin{aligned}\mathrm{E}\left[x_i^2 \mid \mathbf{L}_i^{flag}\right] &= \sum_{s=0}^{q-1} \lambda_s^2 \mathrm{Prob}\left[x_i = \lambda_s\right] \\ &= \frac{\sum_{s=0}^{q-1} \lambda_s^2 \exp\left(L_{i,s}\right)}{\sum_{t=0}^{q-1} \lambda_t^2 \exp\left(L_{i,t}\right)}\end{aligned} \tag{18}$$

After the filtering operation as (4), an equivalent single input single output channel with input x_k and output $\hat{x}_k$ can also be derived as formula (10). The component-wise *a posteriori* LLRs of the transmitted symbol (I/Q branch) x_k can be calculated as follows [8]

$$\begin{aligned}L_{\mathrm{det}}^{post}\left(x_k = \chi(\alpha)\right) &= \ln \frac{p(x_k = \chi(\alpha) \mid \hat{x}_k)}{p(x_k = \chi(0) \mid \hat{x}_k)} \\ &= \ln \frac{p\left(\hat{x}_k \mid x_k = \chi(\alpha)\right) \cdot p\left(x_k = \chi(\alpha)\right)}{p\left(\hat{x}_k \mid x_k = \chi(0)\right) \cdot p\left(x_k = \chi(0)\right)} \\ &= \underbrace{\ln \frac{p\left(\hat{x}_k \mid x_k = \chi(\alpha)\right)}{p\left(\hat{x}_k \mid x_k = \chi(0)\right)}}_{extrinsic\ \mathrm{LLR}} + \underbrace{\ln \frac{p\left(x_k = \chi(\alpha)\right)}{p\left(x_k = \chi(0)\right)}}_{a\ priori\ \mathrm{LLR}}\end{aligned} \tag{19}$$

where $\alpha \in \mathrm{GF}(q)$, $\chi(\cdot)$ denotes the mapping from GF(q) symbol to constellation point, take 16-QAM with partial mapping for example, $\chi(0) = -3.0/\sqrt{10}$, $\chi(1) = -1.0/\sqrt{10}$, $\chi(2) = 3.0/\sqrt{10}$, $\chi(3) = 1.0/\sqrt{10}$. Let $\mathbf{L}_{\mathrm{det}}^{post} = \left[L_{\mathrm{det}}^{post}\left(x_k = \chi(0)\right), \cdots, L_{\mathrm{det}}^{post}\left(x_k = \chi(q-1)\right)\right]$ denotes q *a posteriori* LLRs values and $\mathbf{L}_{\mathrm{det}}^{ext} = \left[L_{\mathrm{det}}^{ext}\left(x_k = \chi(0)\right), \cdots, L_{\mathrm{det}}^{ext}\left(x_k = \chi(q-1)\right)\right]$ denotes extrinsic LLRs of a GF(q) symbol associated with x_k. For $0 \le \alpha \le q-1$, the associated extrinsic LLR can be calculated as follows:

$$\begin{aligned}L_{\mathrm{det}}^{ext}\left(x_k = \chi(\alpha)\right) &= \ln \frac{p\left(\hat{x}_k \mid x_k = \chi(\alpha)\right)}{p\left(\hat{x}_k \mid x_k = \chi(0)\right)} \\ &= -\ln \frac{\left(\hat{x}_k - \tau\chi(\alpha)\right)^2}{2\sigma_z^2} + \ln \frac{\left(\hat{x}_k - \tau\chi(0)\right)^2}{2\sigma_z^2}\end{aligned} \tag{20}$$

Let $\mathbf{L}_{\mathrm{det}}^{ext} = \left[L_{\mathrm{det}}^{ext}\left(x_k = \chi(0)\right), \cdots, L_{\mathrm{det}}^{ext}\left(x_k = \chi(q-1)\right)\right]$ and $\gamma = \max\left(\mathbf{L}_{\mathrm{det}}^{ext}\right)$. To improve the numerical stability, the following operation was introduced for all $\alpha \in \mathrm{GF}(q)$,

$$\hat{L}_{\mathrm{det}}^{ext}\left(x_k = \chi(\alpha)\right) = L_{\mathrm{det}}^{ext}\left(x_k = \chi(\alpha)\right) - \gamma \tag{21}$$

where $\hat{L}_{\mathrm{det}}^{ext}\left(x_k = \chi(0)\right) = 0$.

3.4 MSE based ordering for CLSIC-LMMSE based MUD

After x_k is detected, the index of the next symbol to be detected can be determined according to (22).

$$k+1=\underset{n\notin\{1,2,\cdots,k\}}{\arg\min}\,\mathrm{E}\left(\left|x_n-\hat{x}_n\right|^2\right)$$
$$=\underset{n\notin\{1,2,\cdots,k\}}{\arg\min}\,\mathrm{E}\left(\left|x_n\right|^2\right)\left(1-\mathrm{var}\left(x_n\right)\mathbf{h}_n^H\left(\mathbf{H}R_{xx}{}^H+\sigma^2\mathbf{I}_{n_r}\right)^{-1}\mathbf{h}_n\right) \quad (22)$$

where $\mathrm{var}(x_k)=0.5$, $\mathbf{I}_{2N_r}$ denotes $2N_r\times 2N_r$ identity matrix and $\mathbf{h}_n$ denotes the n-th column of matrix $\mathbf{H}$. Take the detection of MU-MIMO system with $N_t=4$ and $N_r=4$ for example, as shown in **Fig. 3**, for $1\le i\le N_t$, the symbol-wise MSE metric d_i of symbol x_i can be decomposite into two tuples $\left(d_{i,I}^2,d_{i,Q}^2\right)$, where $d_{i,I}^2$ and $d_{i,Q}^2$ denote the in-phase component and quadrature metrics respectively and $d_i=d_{i,I}^2+d_{i,Q}^2$. Since the symbol metrics d_x = d_z, the SLSIC-LMMSE MUD will choose either symbol x or z for detection randomly. However, for CLSIC-LMMSE-based MUD, it will choose the in-phase component of x for detection due to $d_{x,I}^2<d_{x,Q}^2$, $d_{x,I}^2<d_{z,I}^2$ and $d_{x,I}^2<d_{z,Q}^2$. Furthermore, as shown in **Fig. 3**, although the symbol-wise MSE of x is larger than that of y, the CLSIC-LMMSE-based MUD can also choose the component x_I for detection since it is the least one among $d_{x,I}^2$, $d_{x,Q}^2$, $d_{y,I}^2$ and $d_{y,Q}^2$. Compared with SLSIC-LMMSE-based MUD, the CLSIC-LMMSE-based one can choose the component with the least MSE metric for detection under all situations, thus reducing error propagation.

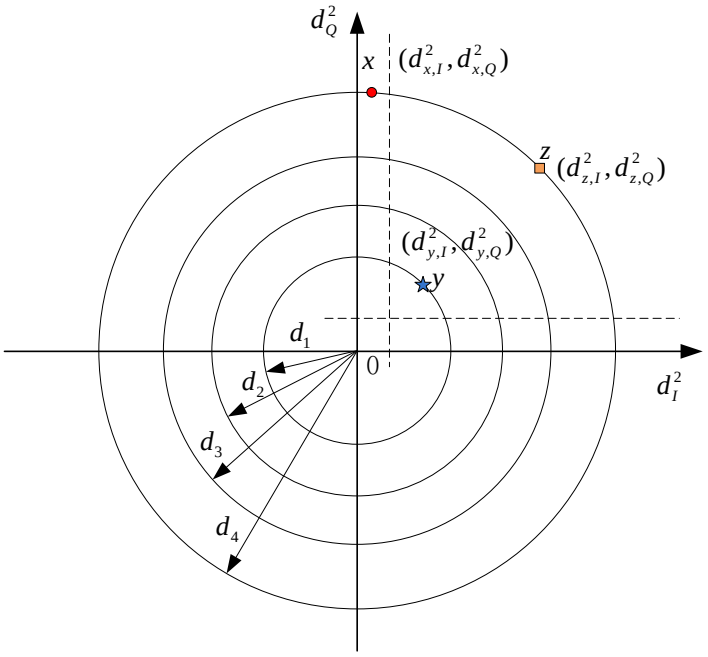

Fig. 3. MSE based ordering

In order to describe the algorithm more clearly, the iterative procedure of CLSIC-LMMSE algorithm is shown in Algorithm 1 as follows:

Algorithm 1: CLSIC-LMMSE-based MUD (N_t users)

1: **if** $k < 2N_t$
2: Choose the user with the MMSE for detection according to (22), e.g. x_k.
3: Calculate soft symbols according to (12) and (13) (or (17) and (18)).
4: Perform CLSIC operation according to (5).
5: Calculate $\boldsymbol{w}_k$ according to (7), and perform LMMSE filtering as (4).
6: Calculate bit-wise LLRs/component-wise LLR according to (16)/(21) for turbo/nonbinary LDPC coded system respectively.
7: **endif**

4. EXIT chart analysis and Numerical simulation results

4.1 EXIT chart analysis for turbo coded MU-MIMO systems

In this section, EXIT chart [3, 10] is employed to analyze the convergence behavior of aforementioned two kinds of detectors. Let I_{det}^{apri} and I_{det}^{ext} denote the average mutual information (AMI) at the input and output of the MIMO detector. Similarly, I_{dec}^{apri} and I_{dec}^{ext} are AMI at the input and output of the channel decoder respectively. To draw the EXIT charts, as shown in Fig.4, we need to calculate the output I_{det}^{ext} for each input I_{det}^{apri} for $I_{\text{det}}^{apri} \in [0:1]$. I_{det}^{apri} will be chosen at the interval of 0.01 to reduce the computation complexity. Similarly, we also need to calculate the output I_{dec}^{ext} for each input I_{dec}^{apri}, where $I_{\text{dec}}^{apri} \in [0:1]$, I_{dec}^{apri} also be chosen at the interval of 0.01. According to the Gaussian approximation method proposed in [11], *a priori* LLR A can be modeled as:

$$A = \mu_A x + n_0 \tag{23}$$

where $x \in \{\pm 1\}$, $n_0 \sim N\left(0, \sigma_0^2\right)$, $\mathrm{E}\left(\mu_A\right) = \sigma_0^2 / 2$, $\mathrm{var}(A) = \mathrm{var}\left(n_0\right) = \sigma_0^2$. Thus, the average mutual information (AMI) between the transmitted symbol x and *a priori* LLR A can be calculated as

$$I(x;A) = J(\sigma) = 1 - \frac{1}{\sqrt{2\pi}\sigma} \int_{-\infty}^{+\infty} \exp\left(-\frac{\left(\xi - \left(\sigma^2/2\right)\right)^2}{2\sigma^2} \right) \log_2(1 + e^{-\xi}) d\xi \tag{24}$$

for each $I_{\text{det}}^{apri} \in [0:1]$, the *a priori* LLR A can be modeled as equation (23), where $\sigma = J^{-1}\left(I_{\text{det}}^{apri}\right)$, $n_0 \sim N\left(0, \sigma_0^2\right)$ and $\mathrm{E}\left(\mu_A\right) = \sigma_0^2 / 2$. Furthermore, the output AMI can be computed as:

$$I_{\text{det}}^{ext} = I\left(x; L_{k,\beta}^{ext}\right) = \frac{1}{2} \sum_{x \in \{\pm 1\}} \int_{-\infty}^{+\infty} p_E\left(L_{k,\beta}^{ext} \mid X = x\right) \log_2 \frac{2 \times p_E\left(L_{k,\beta}^{ext} \mid X = x\right)}{p_E\left(L_{k,\beta}^{ext} \mid X = -1\right) + p_E\left(L_{k,\beta}^{ext} \mid X = +1\right)} d\xi \tag{25}$$

Fig. 4(a) shows the EXIT charts of the CLSIC-LMMSE-based MUD and that of the SLSIC-LMMSE-based one [8], both of which with Gray-mapping based QPSK constellation and E_b/N_0=3dB. The EXIT curve of CLSIC-LMMSE-based MUD positioned above that of SLSIC-LMMSE-based one. The wider tunnel of the CLSIC-LMMSE-based MUD indicates

that the system with the CLSIC-LMMSE-IDD has faster convergence speed and better BER performance. **Fig. 4(b)** shows the EXIT charts of both iterative receivers with 16QAM and E_b/N_0 is 10dB. Similar phenomenon as that of the QPSK is observed for the 16QAM case. Furthermore, we can see from these two figures that the improvement of performance is more pronounced for high order modulation.

4.2 Numerical simulation result for turbo coded MU-MIMO systems

In this subsection, the performance of the proposed CLSIC-LMMSE-based iterative receiver is compared with SLSIC-LMMSE-based one. We consider a turbo-coded MIMO-OFDM multiplexing system with 1024-point fast Fourier transform (FFT) and 15KHz subcarrier spacing. At the transmitter side, binary source bits are encoded with turbo code fisrtly. Then coded bits are interleaved and modulated.

The turbo code with original code rate R_c=1/3 (generators polynomial $[13, 18]_8$) and then punctured according to code rate R_c=1/2 and R_c=5/6 as specified in [12]. The number of outer iteration performed between MUD and turbo decoder is denoted by *It_out*, while the number of inner iteration of turbo decoder is denoted by *It_in*. In this paper, all turbo codes with fixed number of inner iteration, i.e., *It_in*=2, the number of outer iteration is marked in the figures plotted. **Fig. 5(a)** and **Fig. 5(b)** show the BER performance of the proposed CLSIC-LMMSE based IDD receivers both with turbo code of rate R_c=1/2. In **Fig. 5(a)**, under QPSK modulation, the BER performance of the CLSIC-LMMSE-IDD receiver is compared with that of the SLSIC-LMMSE-IDD in the same setting.

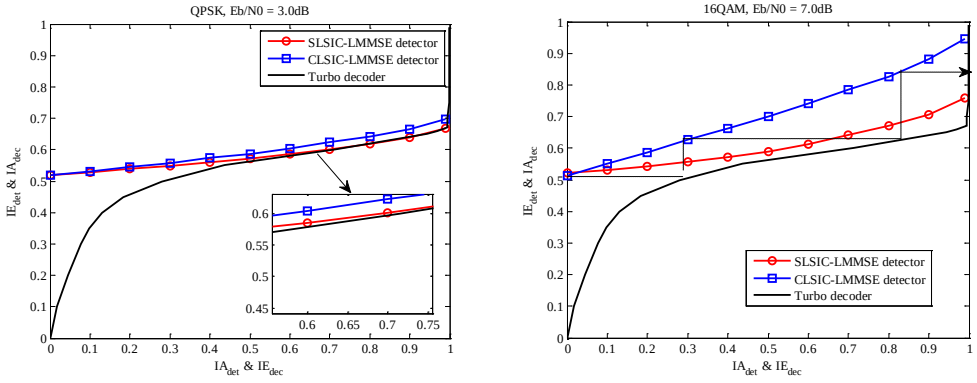

(a) (b)

Fig. 4. EXIT Comparisons between CLSIC-LMMSE based detector and SLSIC-LMMSE based one

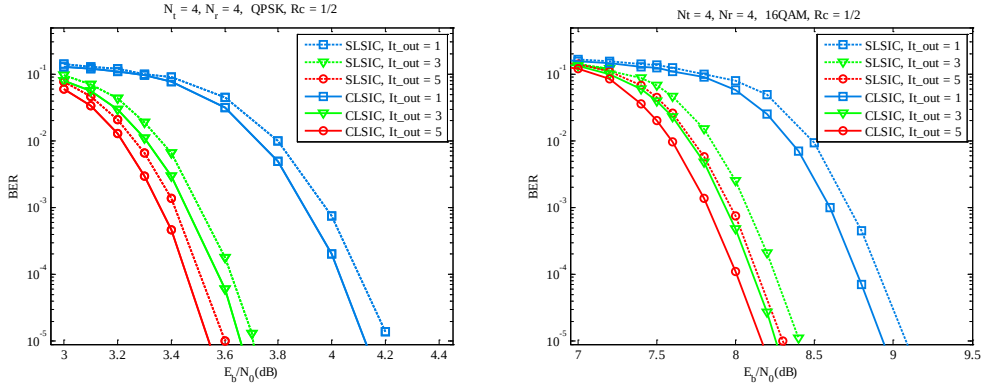

(a) (b)

Fig. 5. Performance comparisons between both schemes with R_c=1/2

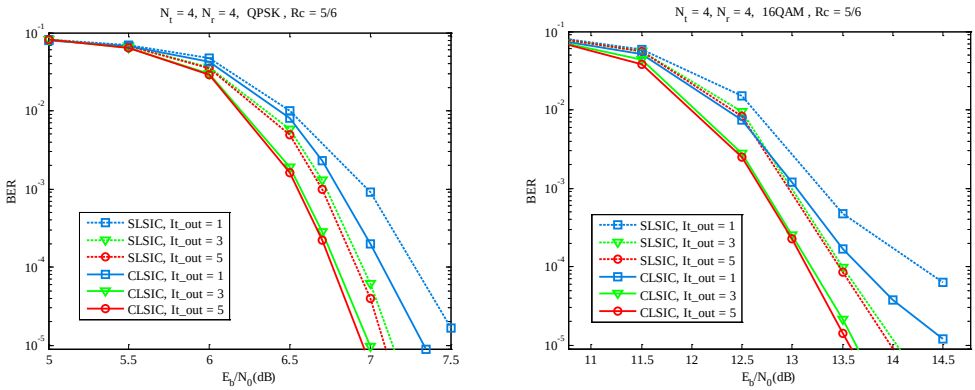

(a) (b)

Fig. 6. Performance comparisons between both schemes with R_c=5/6

The performance gain is 0.05dB at BER=1×10^{-5} with *It_out*=5. For 16QAM case, as is plotted in **Fig. 5(b)**, a performance gain of about 0.25dB is obtained at BER=1×10^{-5}. For high code rate R_c=5/6, the performance gain is 0.15dB and 0.5dB respectively for QPSK and 16QAM, as shown in **Fig. 6(a)** and **Fig. 6(b)** respectively. For all cases of interest, the CLSIC-LMMSE-based IDD receiver outperforms the SLSC-LMMSE-based one.

4.3 EXIT chart analysis for non-binary LDPC coded MU-MIMO systems

In this subsection, non-binary AMI chart [7], is employed to analyze the convergence behavior of both schemes. In **Fig. 7**, IA_{det} and IE_{det} denote the average mutual information at the input and output of the MIMO detector. To draw the AMI chart of the MIMO detector, we need to calculate the output IE_{det} for each input IA_{det}, and can be expressed as IE_{det} (IA_{det}). For the purpose of reducing the computational complexity, IA_{det} was selected at the interval of 0.05 between 0 and 1. In [7,13], the *a priori* LLR-vector are approximated by q-1 dimensional vector $\mathbf{W}=(w_1,\ldots,w_{q-1})$ associated with $x=0$ is transmitted. Let $\mathbf{W}$ denote a Gaussian random vector with mean vector $\mathbf{m}$ and covariance matrix $\mathbf{D}$, where

$$\mathbf{m}=\begin{bmatrix}-\sigma^2/2\\-\sigma^2/2\\\vdots\\-\sigma^2/2\end{bmatrix} \qquad \mathbf{D}=\begin{bmatrix}\sigma^2 & & & \sigma^2/2\\ & \sigma^2 & & \\ & & \ddots & \\ \sigma^2/2 & & & \sigma^2\end{bmatrix} \tag{26}$$

For $x=\alpha$, the associating *a priori* LLR can be modeled as:

$$\mathbf{L}=\mathbf{W}^{-\alpha}=\begin{bmatrix}w_{0-\alpha}-w_{-\alpha}\\w_{1-\alpha}-w_{-\alpha}\\\vdots\\w_{q-1-\alpha}-w_{-\alpha}\end{bmatrix}_{q\times q}\cong\begin{bmatrix}w_{1-\alpha}-w_{-\alpha}\\w_{2-\alpha}-w_{-\alpha}\\\vdots\\w_{q-1-\alpha}-w_{-\alpha}\end{bmatrix}_{(q-1)\times(q-1)} \tag{27}$$

The last equality is obtained by eliminating the first row of the $q\times q$ matrix since $W_{0-\alpha}-W_{-\alpha}=0$. According to [14], after $\mathbf{L}_{\text{det}}^{ext}$ obtained by monte carlo simulation, the AMI

between the extrinsic information $\mathbf{L}_{\text{det}}^{ext}$ and the transmitted symbol $\mathbf{x}$ can be calculated as follows:

$$I_{\text{det}}^{ext} = I\left(\boldsymbol{x};\mathbf{L}_{\text{det}}^{ext}\right) = H\left(x\right) + \mathrm{E}\left\{\frac{1}{N_s}\sum_{l=0}^{N_s-1}\sum_{\alpha=0}^{q} p\left(x_l, L_{\text{det}}^{ext}\right)\log_2 p\left(x_l, L_{\text{det}}^{ext}\right)\right\} \tag{28}$$

where $H\left(x\right) = -p\left(x\right)\log_2 P\left(x\right) - \left(1-P\left(x\right)\right)\log_2\left(1-P\left(x\right)\right)$ denotes the entropy funciton and $0 \le H\left(x\right) \le 1$, q is the order of the GF. From **Fig. 7**, the major observations can be listed as follows:

- Since IA_{det}=0 corresponding to the case without IDD. For SLSC-LMMSE-based scheme, $IE_{det}(0)$=0.8119 at E_b/N_0=10.0dB. While for CLSC-LMMSE-based scheme, $IE_{det}(0)$=0.8119 at E_b/N_0=9.8dB. It means that the CLSC-LMMSE-based MUD detector outperform the SLSC-LMMSE-based one 0.2dB when both schemes without IDD.
- The AMI chart of CLSC-LMMSE-based IDD receiver with larger slope than that of SLSC-LMMSE-based one, indicating that the former with potentially larger iterative gain.

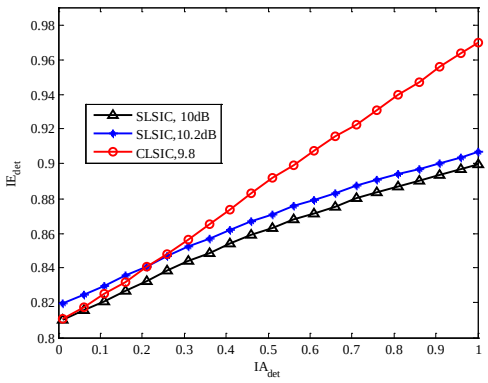

Fig. 7. AMI chart analysis for both MUDs

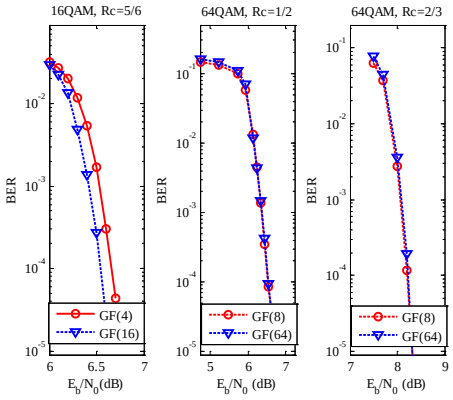

Fig. 8. Performance of construced nonbinary LDPC codes under AWGN channel

4.4 Numerical simulation result for non-binary LDPC coded MU-MIMO system

In order to compare the performance of the proposed CLSIC-LMMSE-based MUD with the conventional SLSIC-LMMSE-based one, take 16QAM for example, two LDPC codes over GF(2^2) and GF(2^4) with approximately the same performance are constructed respectively. The former is used for CLSIC-LMMSE-based system and the latter is used for SLSIC-LMMSE-based system, and both systems with 16QAM. As shown as code 1 and code 2 in **Table 1**, the primitive polynomials used to generate GF(2^2) and GF(2^4) are $g(\alpha) = 1+\alpha+\alpha^2$ and $g(\alpha) = 1+\alpha+\alpha^4$ respectively, where α is the primitive element [15]. The code over GF(2^2) with code length N_s = 4800 and information symbols length K_s = 4000, while the code over GF(2^4) with N_s = 2400 and K_s = 2000. Both codes with rate R_c = 5/6 and with bit-wise length N_b = 9600. The GF(2^2)-LDPC code (Code 1) with regular degree distributions (column weight 3 and row weight 18) while the GF(2^4)-LDPC code (Code2) with variable node degree distribution $\lambda(x) = 0.25x + 0.75x^2$ and check node degree distribution $\rho(x) = x^{15}$, both codes constructed by replacing the nonzero entries in binary mask matrix with

randomly-selected nonzero elements in GF(q). **Fig. 8(a)** shows the BER performance of these two codes with 16-QAM and ML demodulation under AWGN channel. The number of LDPC decoding iterations is set to 30. The GF(2^4)-LDPC code outperforms the GF(2^2)-LDPC code approximately 0.1dB at the BER level of 1×10^{-4}. Here we do not intend to show the good performance of the codes that we constructed, but provide two non-binary LDPC codes with approximately the same error correcting performance. Similarly, code 3 and code4 are all of rate R_c = 1/2 used for CLSIC-LMMSE-IDD and SLSIC-LMMSE-IDD system with 64QAM respectively, code 5 and code 6 are all of rate R_c = 2/3 used for CLSIC-LMMSE-IDD and SLSIC-LMMSE-IDD system with 64QAM respectively.

Table 1. The parameters of used non-binaryLDPC codes

Code	Galois field	Primitive polynomial	Degree distribution	Code length	Code rate
Code 1	GF(4)	$g(\alpha)=1+\alpha+\alpha^2$	$\lambda(x)=x^2$ $\rho(x)=x^{17}$	$N_s=4800$ $N_b=9600$	R_c=5/6
Code 2	GF(16)	$g(\alpha)=1+\alpha+\alpha^4$	$\lambda(x)=0.25x+0.75x^2$ $\rho(x)=x^{15}$	$N_s=2400$ $N_b=9600$	R_c=5/6
Code 3	GF(8)	$g(\alpha)=1+\alpha+\alpha^3$	$\lambda(x)=0.1x+0.9x^2$ $\rho(x)=0.25x^4+0.75x^5$	$N_s=3600$ $N_b=9600$	R_c=1/2
Code 4	GF(64)	$g(\alpha)=1+\alpha+\alpha^6$	$\lambda(x)=0.4x+0.6x^2$ $\rho(x)=x^4$	$N_s=1600$ $N_b=9600$	R_c=1/2
Code 5	GF(8)	$g(\alpha)=1+\alpha+\alpha^3$	$\lambda(x)=0.1x+0.9x^2$ $\rho(x)=0.4x^7+0.6x^8$	$N_s=3600$ $N_b=9600$	R_c=2/3
Code 6	GF(64)	$g(\alpha)=1+\alpha+\alpha^6$	$\lambda(x)=0.5x^5+0.5x^5$ $\rho(x)=0.64x^7+0.36x^8$	$N_s=1600$ $N_b=9600$	R_c=2/3

At the transmitter, source bits are encoded with non-binary LDPC code. Then the output code-word is interleaved and modulated. For clarity, the number of outer iteration performed between MUD and non-binary LDPC decoder is denoted by *Out_it*, and the number of inner iteration of non-binary LDPC decoder is denoted by *In_it*. In this work, all non-binary LDPC codes with fixed number of inner iteration *In_it* = 30, and the number of outer iterations is marked in the figures plotted. In **Fig. 9**, the performance of the proposed CLSIC-LMMSE-based IDD is compared with that of the SLSIC-LMMSE-based one under the condition that both schemes with N_t = N_r = 4 and 16-QAM. We have the following observations:

- Without IDD, if the same channel coding (GF(2^2)-LDPC code) scheme is used , the proposed CLSIC-LMMSE-based MUD outperform the SLSIC-LMMSE-based one 0.2dB as shown in **Fig. 9(a)**, this coincide with the aforementioned non-binary AMI chart analysis as shown if **Fig. 7**;

- Compared with the SLSIC-LMMSE-IDD, as shown in **Fig. 9(b)**, the proposed CLSIC-LMMSE-IDD receiver has a performance gain about 0.2dB with *Out_it* = 1. As the number of outer iterations increase, e.g., *Out_it* = 5, the performance gain is about

0.9dB at BER=1×10^{-5}, c) the proposed CLSIC-LMMSE-IDD scheme with *Out_it* = 5 only worse than ML based one about 1.3dB.

- With *Out_it* = 5 and R_c =5/6, Compared with the turbo coded MU-MIMO system as shown in **Fig. 6 (b)**, the GF(4)-LDPC coded MU-MIMO system achieves about 1dB peformance gain as shown in **Fig. 9(b)**.

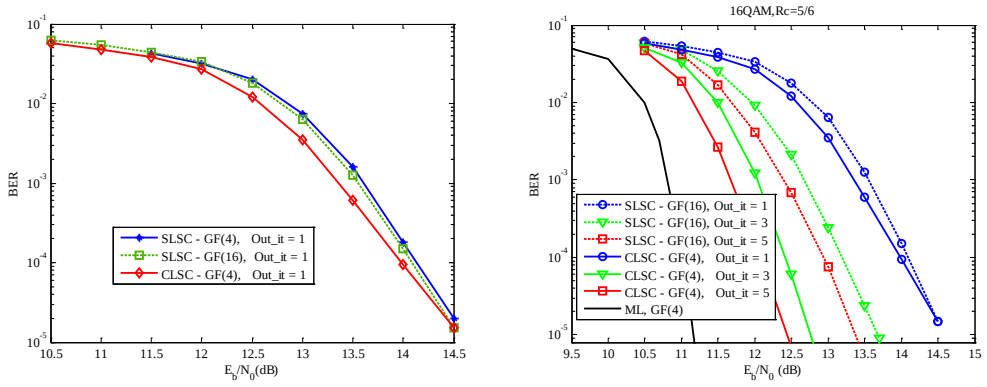

(a) (b)

Fig. 9. Peformance comparison between both schemes in 16QAM system

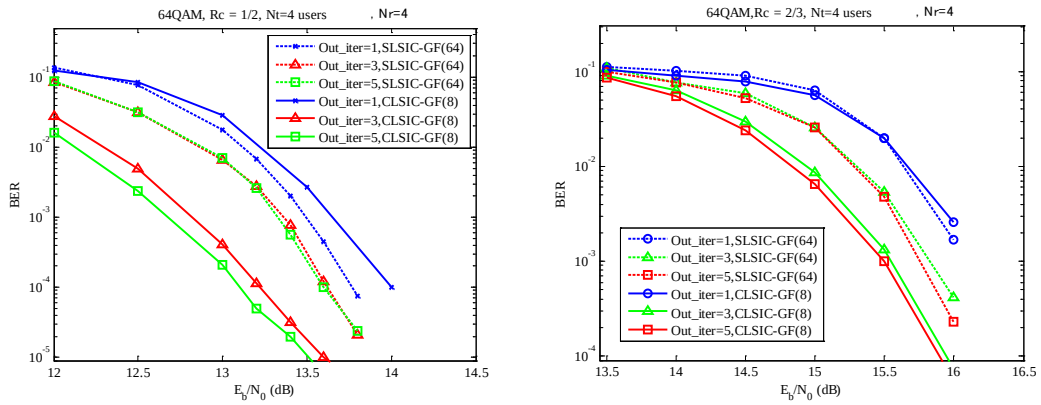

(a) (b)

Fig. 10. Peformance comparisons between both schemes in 64QAM systems

Fig. 10 shows the simulation results for the cases of 64QAM with non-binary LDPC codes of rate R_c = 1/2 and R_c = 2/3 respectively. For CLSIC-LMMSE-based MUD, the GF(8)-LDPC and partial mapping is employed which is similar to **Fig. 2(b)**, while for SLSIC-LMMSE-based MUD, the GF(64)-LDPC and partial mapping is employed which is similar to **Fig. 2(a)** for comparison purposed. For both code rates, the proposed GF(8)-LDPC coded MIMO system with CLSIC-LMMSE-IDD not only achieves about 0.5dB performance gains over GF(64)-LDPC coded MIMO system with SLSIC-LMMSE-IDD but also with lower complexity as shown in the next subsection.

4.5 Complexity comparison

In this work, forward-backward (FB) based log-domain belief propagation (Log-BP) algorithm [8] is employed to decode the non-binary LDPC codes. Since the check node update is the bottleneck of the decoding complexity, we only need to compare the computational complexity of the elementary check node (ECN) processing. According to [16], take 16QAM system for example [17-18], the decoding complexity of GF(2^2)-LDPC code is about only 1/8 or 1/4 of GF(2^4)-LDPC code under log-BP or FFT-BP decoding respectively as shown in **Table 2**. Moreover, for 64QAM cases, the GF(2^3)-LDPC coded systems can achieve 0.5dB BER performance gain over GF(2^6)-LDPC coded ones while the former with about 1/32 and 1/8 decoding complexity of the later one. Significantly performance reduction is the main motivation of the proposed schemes.

Table 2. Comparisons between CLSIC-LMMSE-based scheme and SLSIC-LMMSE-based one

Modulation and code-rate		BER Performance gain	Comparisons of compl-exity under Log-BP decoding algorithm	Comparison of compl-exity under FFT-BP decoding algorithm
16QAM	R_c = 5/6	1dB	1:8	1:4
64QAM	R_c =1/2	0.5dB	1:32	1:8
	R_c =2/3	0.5dB		

5. Conclusion

In this paper, we first proposed a CLSIC-LMMSE-based MUD algorithm for MU-MIMO system. By exploiting the independence of the in-phase and quadrature components, the soft symbol of each detected component can be canceled more efficiently. For binary turbo coded MIMO system, the proposed MUD algorithm achieves better performance gain over traditional SLSIC-LMMSE-based one under different code rates and modulation formats. Furthermore, a non-binary LDPC coded MU-MIMO scheme combined with partial mapping is presented to achieve good performance and complexity tradeoffs for high order modulation systems. It not only enhances the MUD performance but also reduces the decoding complexity significantly, which make the non-binary LDPC coded high order modulation scheme for MIMO systems attractive for complexity-constrained applications.

References

[1] Jeongwook Seo, Won-Gi Jeon, Jong-Ho Paik and Dong Ku Kim, "A Composite LMMSE Channel Estimator for Spectrum-Efficient OFDM Transmit Diversity," *KSII Transactions on Internet and Information Systems*, Vol. 2, No. 4, pp.209-221, Aug. 2008. Article (CrossRef Link)

[2] S. Pfletschinger, D. Declercq, "Getting Closer to MIMO Capacity with Non-Binary Codes and Spatial Multiplexing," in *Proc. of IEEE GLOBECOM 2010*, pp.1-5, Dec. 6-10, 2010. Article (CrossRef Link)

[3] S. Brink, G. Kramer, A. Ashikhmin, "Design of low-density parity check codes for modulation and detection," *IEEE Trans. Commun.*, vol. 52, no. 4, pp. 670-678, Apr. 2004. Article (CrossRef Link)

[4] H. Kwon, J. lee and I. Kang, "Successive Interference Cancellation via Rank-Reduced Maximum A posteriori Detection," *IEEE Trans. Commun.*, vol. 61, no. 2, pp. 628-637, Feb. 2013. Article (CrossRef Link)

[5] H. lee, B. Lee, and I. Lee, "Iterative detection and decoding with an improved V-BLAST for MIMO-OFDM systems," *IEEE J. Sel. Areas Commun.*, vol. 24, no. 3, pp. 504-513, Mar. 2006. Article (CrossRef Link)
[6] J. W. Choi, A. C. Singer, and J. lee, "Improved Linear Soft-Input Soft-output Detection via Soft Feedback Successive Interference Cancellation," *IEEE Trans. Commun*., vol. 58, no. 3, pp. 986-996, Mar. 2010. Article (CrossRef Link)
[7] A. Bennatan and D. Burshtein, "Design and analysis of non-binary LDPC codes for arbitrary discrete memoryless channels," *IEEE Trans. Inf. Theory*., vol. 52, no. 2, pp. 549-583, Feb. 2006. Article (CrossRef Link)
[8] H. Wymeersch, H. Steendam, and M. Moeneclaey, "Log-domain decoding of LDPC codes over GF(q)," in *Proc. of IEEE intern. Conf. on Commun.*, pp.772-776, June 20-24, 2004. Article (CrossRef Link)
[9] S. Nowak, G. Seietanka, R. Kays, "High Efficiency Broadband Transmission with LDPC Codes over GF(2^s)," in *Proc. of IEEE International Symposium on Broadband Multimedia Systems and Broadcasting*, pp. 1-6, June 8-10, 2011. Article (CrossRef Link)
[10] M. EI-Hajjar, L. Hanzo, "EXIT charts for system design and analysis," *IEEE Communications Surveys & Tutorials*, vol. 16, no. 1, pp. 127-153, Feb. 2014. Article (CrossRef Link)
[11] S. Y. Chung, T. J. Richardson and R. Urbanke, "Analysis of sum-product decoding of low-density parity-check codes using a Gaussian approximation," *IEEE Trans. Information Theory*, vol. 47, no. 2, Feb. 2001. Article (CrossRef Link)
[12] 3rd Generation Parternship Project, "Technical Specification Group Radio Access Network; Evolved Universal Terrestrial Radio Access (EUTRA); Multiplexing and channel coding," *3GPP TS 36.212 V9.1.0* Mar. 2010.
[13] G. Li, W. A. Krzymien, "Density evolution for nonbinary LDPC codes under Gaussian approximation," *IEEE Trans. Information Theory*, vol. 55, no. 3, pp. 997-1015, Mar. 2009. Article (CrossRef Link)
[14] J. Kliewer, S. X. Ng, L. Hanzo, "Efficient Computation of EXIT Functions for Non-binary Iterative Decoding," *IEEE Trans. Commun.*, vol. 54, no. 12, pp. 2133-2136, Dec. 2006. Article (CrossRef Link)
[15] W. E. Ryan and S. Lin, Channel codes: classic and modern. Cambridge University Press, 2009.
[16] L. Conde-Canencia, A. A. Ghouwayel and E. Boutillon, "Complexity comparison of non-binary LDPC decoders," in *Proc. of ICT-Mobile Summit Conference*, pp. 1-8, June 10-12, 2009.
[17] Jin Xu, et al. "A low-complexity CLSC-LMMSE detection algorithm for non-binary LDPC coded MIMO system," *Journal of Computational Information Systems*, vol. 11, no. 7, pp. 2337-2344, April 2015. Article (CrossRef Link)
[18] J. Xu, et al. "A component-level soft interference cancellation based iterative detection algorithm for coded MIMO systems," in *Proc. of IEEE Vehicular Technology Conference*, pp. 1-5, Sept. 14-17, 2014. Article (CrossRef Link)

Jin Xu received the B.E. degree in Electronics and Information Engineering from Zhengzhou University in 2005 and the M.S. degree in communication and information system from Wuhan University of Technology in 2011 respectively, and the Ph.D. degree in Beijing University of Posts and Telecommunications, Beijing, China in 2015. His research interests include LDPC code, iterative decoding algorithm, MIMO detection, and non-orthogonal multiple access.

Kai Zhang received the B.E degree in Electronics and Information Engineering from Jilin University in 2005 and received the M.S. degree in communication and information system from Beijing University of Posts and Telecommunications in 2009. He is currently pursuing the Ph.D. degree in Beijing University of Posts and Telecommunications, Beijing, China. His research interests include MIMO-OFDM, stochastic geometry.